Research Square

Preprints are preliminary reports that have not undergone peer review.
They should not be considered conclusive, used to inform clinical practice,
or referenced by the media as validated information.

# Exploration of the Relationship Between Bladder Function and Serum Metabolites in Rats with Spinal Cord Injury

**Yinbo Kang**
The First Hospital of Shanxi Medical University
**Yi Rong**
The First Hospital of Shanxi Medical University
**Jie Wen**
The First Hospital of Shanxi Medical University
**Wenlong Zhang**
The First Hospital of Shanxi Medical University
**Qian Gong**
The First Hospital of Shanxi Medical University
**Dingyang Lv**
The First Hospital of Shanxi Medical University
**Huiyu Zhou**
The First Hospital of Shanxi Medical University
**Ke Sun**
The First Hospital of Shanxi Medical University
**Weibing Shuang**
shuangweibing@126.com

The First Hospital of Shanxi Medical University

**Research Article**

**Keywords:** spinal cord injury, serum metabolomics, differential metabolites, bladder function

**Posted Date:** November 10th, 2026

**DOI:** https://doi.org/10.21203/rs.3.rs-11385183/v1

**License:** This work is licensed under a Creative Commons Attribution 4.0 International License.
Read Full License

**Additional Declarations:** No competing interests reported.

# Exploration of the Relationship Between Bladder Function and Serum Metabolites in Rats with Spinal Cord Injury

**Yinbo Kang[1,2·], Yi Rong[1,2·], Jie Wen[1,2·], Wenlong Zhang[1,2], Qian Gong[1,2], Dingyang Lv[1,2], Huiyu Zhou[1,2], Ke Sun[1,2] and Weibing Shuang[1*]**

1. Department of Urinary Surgery, The First Hospital of Shanxi Medical University, Shanxi 030000, China
2. First Clinical Medical College, Shanxi Medical University, Shanxi 030000, China

*Corresponding Author: Weibing Shuang, Email: shuangweibing@126.com

**ABSTRACT: Background:** Spinal cord injury (SCI) often leads to neurogenic bladder dysfunction, which severely impacts patients' quality of life. Metabolic study is closely linked to the pathological progression of SCI and organ dysfunction, but the serum metabolic signatures associated with bladder function impairment after SCI remain unclear. This study aimed to analyze untargeted serum metabolites in SCI rats, explore dynamic metabolic changes at different post-injury time points, and identify potential metabolite biomarkers correlated with bladder muscle function. **Methods:** 72 Serum samples were collected from SCI rats at different time points post-injury and from sham-operated control rats. Liquid chromatography-mass spectrometry (LC-MS) was used for untargeted metabolomic profiling. Unsupervised principal component analysis (PCA) was performed to evaluate the overall sample distribution and analytical stability. Bladder muscle function was assessed using in vitro bladder muscle strip contraction experiments. **Results:** 8 differentially expressed metabolites in SCI rats across different time points compared with controls: asaraldehyde, 4-aminohippuric acid,4-(octyloxy)benzoic acid,syringic acid,23-norcholic acid,xanthurenic acid, 3-hydroxyanthranilic acid (3-HANA) and 4-acetyl-4-(ethoxycarbonyl)heptanedioic acid. Bladder muscle strip experiments revealed impaired contractile function in SCI rats. Correlation analysis further demonstrated that the decrease in 3-HANA and the increase in syringic acid were probably associated with changes in bladder muscle activity. **Conclusions:** This study identified a panel of serum metabolites with dynamic changes after SCI, among which 3-HANA and syringic acid are probably potential biomarkers linked to bladder muscle dysfunction. These metabolites may not only serve as diagnostic indicators for SCI-related bladder impairment but also provide novel targets for therapeutic intervention.

**Keywords:** spinal cord injury, serum metabolomics, differential metabolites, bladder function

## 1 Introduction

Spinal cord injury (SCI) refers to structural or functional damage to the spinal cord caused by various traumatic and non-traumatic events, constituting a serious central nervous system disease. The global prevalence of traumatic SCI ranges from approximately 236 to 1,298 per million, with an annual incidence of 8 to 246 per million.[1] These variations reflect differences in reporting standards and healthcare systems. Traumatic SCI is a significant cause of neurogenic bladder, with about 70-84% of patients experiencing bladder and urinary tract dysfunction. Kidney complications, including hydronephrosis and renal failure, frequently occur after SCI and represent major contributors to patient mortality.[2] Neurogenic bladder resulting from SCI is a complex lower urinary tract disorder that can impair the bladder, urethra, and other lower cavity organs, leading to severe lower urinary tract symptoms.[3] The early onset of metabolism-related diseases, such as glucose intolerance, insulin resistance, and lipid abnormalities, after SCI suggests issues with glucose and lipid metabolism.Subsequently, spinal cord injury may lead to lower urinary tract dysfunction, sexual dysfunction, intestinal dysfunction, and abnormalities in autonomic nervous reflexes.[4] Therefore, effectively treating neurogenic bladder post-SCI is a critical challenge in medical research. Studies have shown that metabolic changes in bladder tissue occur over time. The levels of various metabolites in muscle tissue significantly change, with a notable increase in the early stages of

spinal shock (reflexless state refers to the temporary loss of reflex activity in the spinal cord below the level of the transection after sudden transection of the spinal cord and loss of connection with the higher central nervous system.), particularly within the first 6 hours. By day 7, spinal shock subsides, and differential metabolite levels decrease rapidly, indicating that reduced bladder capacity due to urinary incontinence mitigates metabolic damage. However, at 2 weeks, the injury worsens again, and metabolite levels alter once more. These metabolomic changes post-SCI provide valuable insights into bladder function.[5]

Metabolomics, a key omics technology complementing genomics, transcriptomics, and proteomics, is a crucial component of systems biology. It aims to investigate changes in metabolites over time in biological systems (e.g., cells, tissues) after stimulation or disturbance. By screening differential metabolites between experimental and control groups, researchers can study the biological processes involved and uncover the mechanisms of life activities. Untargeted metabolomics seeks to detect as many metabolites as possible in biological samples to maximize the discovery of total metabolite information. Liquid chromatography–mass spectrometry (LC-MS), are increasingly used in untargeted metabolomics due to their wide detection range and minimal sample preparation requirements.[6] If substances involved in glucose and lipid metabolism are altered after spinal cord injury (SCI), analyzing these changes alongside bladder function can further explore the pathogenesis of neurogenic bladder.

This study aimed to profile dynamic serum metabolic changes at different time points after spinal cord injury (SCI) using untargeted LC-MS metabolomics, screen key differential serum metabolites associated with SCI progression, and further clarify the correlation between characteristic metabolic alterations and impaired bladder smooth muscle contractile function. The ultimate objective was to identify specific metabolite biomarkers for SCI induced neurogenic bladder dysfunction, so as to provide novel potential diagnostic indicators and therapeutic targets for the functional evaluation and clinical intervention of post-SCI bladder injury.

## 2 Methods

### *2.1 Model Making and Grouping*

72 male rats were used: Sprague-Dawley rats(from Taiyuan, China). The rats were 6-8 weeks old and had body weights of 200 ± 20 g, (mean ± SD),were provided by the Experimental Animal Center of Shanxi Medical University (License No.: SCXK (Jin) 2009-0001). The surgical site and instruments were strictly sterilized, and the spinal cord injury model was established under sterile conditions.[7] All Sprague-Dawley rats were fed ad libitum with a 12-hour light/dark cycle, 60%–80% relative humidity, background noise of 30–50 dB, and a manually controlled ambient temperature of 20–24°C.

This study required a total of 72 rats: 36 rats for the spinal cord injury group and 36 rats for the control group. The specific grouping assignments are as follows:

(1)Sham group(H group): Only the back skin muscle was incised and sutured.

(2)Thoracolumbar spinal cord injury group: The thoracolumbar spinal cord was exposed, and a self-designed experimental bench vertical strike device was used to damage the T10 thoracolumbar spinal cord.Using an impact rod weighing 18 grams dropped from a height of 10 cm, immediate observation revealed convulsions in both lower limbs and tail swaying in the rat, followed by complete relaxation.[8] This group was further divided into six subgroups based on the time after injury: 1 hour (Group A), 6 hours (Group B), 24 hours (Group C), 3 days(Group D), 7 days (Group E), and 14 days (Group G).

Induction anesthesia was performed using 4% isoflurane gas, with animals entering an anesthetic state after approximately 3–5 minutes. Subsequently, anesthesia was maintained using a mask with a mixture of 1% isoflurane gas and 1 L/min oxygen. At the end of the study, rats were euthanized under deep anesthesia via cardiac puncture.

This study was approved by the Animal Experimentation Ethics Committee of Shanxi Medical University and was in accordance with the National Academy of Sciences Guide for the Care and Use of Laboratory Animals (IRB: DWYJ-2024-091).

### *2.2 Sample Extraction*

Rats were anesthetized by inhalation of isoflurane and fixed in the supine position with four limbs immobilized; after depilating the chest and abdomen, the operative region was disinfected three times with iodophor cotton balls, the abdominal skin was lifted with forceps held in the left hand, and a V-shaped small incision was cut with scissors in the right hand while avoiding superficial cutaneous blood vessels, then the incision was extended upward to the xiphoid process to obtain an appropriate operative field. A cotton ball held with forceps was used to push the abdominal viscera to the left to fully expose the vena cava, and the fascia and surrounding tissues around the dark purple vena cava were bluntly dissected with forceps held in both hands; a blood collection needle was inserted at a 30° angle approximately 5 mm deep into the vena cava above its bifurcation at the lower segment, and a vacuum blood collection tube was quickly connected once blood backflow was observed. After blood collection, the whole blood was kept at room temperature for 1–2 hours and centrifuged at 3000 rpm (approximately 1400×g) for 15 minutes, the supernatant serum was transferred into EP tubes with a pipette and stored at −80 °C. For subsequent LC-MS analysis, 100 μL serum sample was transferred to an EP tube and mixed with 400 μL 80% methanol aqueous solution; the mixture was vortexed, incubated on ice for 5 min, and centrifuged at 15,000 g and 4 °C for 20 min, then the collected supernatant was diluted with mass spectrometry-grade water to a methanol concentration of 53%, followed by another centrifugation at 15,000 g and 4 °C for 20 min, and the final supernatant was collected for LC-MS injection.

Quality control (QC) Sample: Mix equal volumes from each experimental sample to create the QC sample.

Blank Sample: Use a 53% methanol water solution instead of the experimental sample, following the same pretreatment process.

### *2.3The mass spectrometric detection*

Chromatographic separation was performed on a Waters ACQUITY UPLC BEH C18 column (1.7 μm, 2.1 mm × 100 mm) maintained at 40 °C with a constant flow rate of 0.3 mL/min. Mobile phase solvent A consisted of ultrapure water containing 0.1% formic acid, and solvent B was acetonitrile supplemented with 0.1% formic acid. The gradient elution procedure was set as follows: 0–2 min, linear gradient from 95% A / 5% B to 90% A / 10% B; 2–6 min, linear gradient from 90% A to 70% A; 6–12 min, 70% A down to 40% A; 12–18 min, 40% A reduced to 10% A; 18–20 min, held at 10% A / 90% B for column washing; at 20 min, the mobile phase was rapidly returned to 95% A / 5% B, and the column was equilibrated at this ratio from 20 min to 24 min before the next injection. The injection volume was 5 μL, and both QC and blank samples were analyzed using the identical gradient program.

The mass spectrometric（Q Exactive-HF-X）detection was operated under electrospray ionization positive ion mode (ESI+). For full scan MS1 and data-dependent MS/MS (ddMS2) acquisition, the Orbitrap mass analyzer was configured with a mass resolution of 120,000 (m/z 200) for MS1 full scan, and 30,000 (m/z 200) for ddMS2 secondary scanning. The normalized collision energy (NCE) for MS/MS fragmentation analysis was set as a stepped value of 20, 40, and 60.[9]

The machine data (.raw) file was imported into Compound Discoverer 3.3 search software for processing. Each metabolite was screened for retention time, mass, charge ratio, and other parameters. The peak area was corrected using QC sample for more accurate identification. Subsequently, peak extraction was performed with a mass deviation of 5 ppm, signal intensity deviation of 30%, minimum signal intensity, adduct ion, and other information. Signal-to-noise ratio (S/N) threshold: 3;Minimum number of scan points per peak: 5;Maximum peak width: 0.25;min Baseline removal: enabled Gap ratio threshold: 0.35.The total ion intensity (TIC) is obtained by summing the peak areas of all detected peaks within a single sample; the corrected area for each peak is calculated as (original peak area ÷ total TIC of that sample) × TIC of the reference sample (with the default reference value being the mean TIC across all samples). This

approach ensures that the total intensity of all characteristic signals in a single sample remains constant.

### *2.4 Mechanical Distraction Stimulation Experiment of Muscle Strips*

Krebs fluid(pH 7.35) contained NaCl 118 mM, KCl 4.75 mM, $MgSO_4$ 1.18 mM, $KH_2PO_4$ 1.18 mM, $NaHCO_3$ 24.8 mM, glucose 10 mM, and $CaCl_2$ 2.5 mM.

A muscle strip which was obtained from rat bladder muscle tissue was prepared by tying both ends with 4/0 suture thread. One end was fixed to the bottom of a fixation plate, while the other end was connected to a thread tension sensor induction head. All muscle strips were placed in an organ bath filled with Krebs fluid and maintained in an organ bath for 30 minutes without tension. During the experiment, the liquid in the organ bath was kept at 37°C using a thermostatic pump. The tank was perfused with a mixed gas containing 95% oxygen and 5% carbon dioxide, and the liquid composition was maintained by constant pressure perfusion.

The pull sensor was connected to a computer via a matching connection, allowing the multimedia biological signal recording and analysis.Multimedia biological signal recording and analysis system (Model BL-420N) was supplied by Chengdu Taimeng Software Co., Ltd., Chengdu, China to detect and record signals. The fine-tuning helix was adjusted to gradually increase the strip tension until 1 to 7 spontaneous contractions per minute were observed, establishing the tension threshold for spontaneous contraction. Once spontaneous contractions were stable for 15 minutes, changes in muscle strip tension were recorded continuously for 45 minutes. The number of phase contraction peaks per minute was recorded as the spontaneous contraction frequency. The contraction amplitude of 10 consecutive contraction peaks was averaged to determine the average contraction force, and the maximum contraction amplitude was recorded as the maximum contraction force.

### *2.5 Statistical Analysis*

We used one-way ANOVA.Post-hoc pairwise comparisons were conducted using the Games–Howell test. on all collected data, which demonstrated statistically significant differences among the indicators. Games-Howell test does not require the assumption of equal variances, was applied, yielding corrected *p*-values and confidence intervals. We used SPSS 27 (IBM Corp., Armonk, NY, USA) to assist with the analysis. (For detailed information, please refer to the supplementary materials.)

Principal component analysis (PCA) is a statistical method that transforms a set of potentially correlated variables into a set of linearly uncorrelated variables through orthogonal transformation. These transformed variables are called principal components. Metabolome data can be considered a multivariate dataset. PCA reduces the dimensionality of metabolite variables by assigning weights through linear combinations, producing new characteristic variables (principal components).The data were log-transformed and normalized using MetaX software 1.4.2. [10-11]

### *2.6 Collection of rat bladder tissue specimens*

After anesthetizing and euthanizing the rats, a midline incision was made in the lower abdominal wall to access the bladder. The bladder was completely isolated, with surrounding fat and connective tissue carefully dissected to avoid damaging the bladder wall epithelium. A longitudinal incision was made along the ventral midline of the bladder; urine within the bladder cavity was gently flushed with normal saline, and excess fluid was absorbed using filter paper. The tissue samples were cut into pieces measuring $\leq$3 mm in thickness and approximately 1 cm × 0.8 cm in dimensions.The bladder wall anatomically consists of four layers (mucosa, submucosa, muscularis, and serosa/adventitia). Within 15 minutes after ex vivo preparation, the samples were immersed in fixation solution. They were labeled, grouped, and numbered to distinguish the tissues of the bladder neck, body, and apex.

The volume of fixed liquid should be at least 10 times that of the tissue, and fixation should be performed at room temperature for 12–24 hours. After fixation, rinse with running water for 30 minutes to remove free formaldehyde and prevent excessive background staining in subsequent staining procedures.

After rinsing, perform gradient ethanol dehydration (70% ethanol for 30 min → 80% ethanol for 30 min → 90% ethanol for 30 min → 95% ethanol twice, each for 20 min → anhydrous ethanol twice, each for 15 min); followed by xylene immersion twice, each for 10 min; then paraffin infiltration at 60°C three times, each for 30 min. Add molten paraffin into the metal mold, place the bladder tissue inside to flatten it, and allow it to cool and solidify.

Paraffin blocks were prepared by refrigerating at 4°C for 30 minutes; sectioned using a rotary microtome to a thickness of 4 μm; mounted on glass slides in a constant temperature water bath at 42°C; sections were mounted onto polylysine-coated anti-desiccation slides for better adhesion; and dried in an oven at 60°C for 60 minutes before dewaxing and storage.

Wax removal: Xylene I for 10 min → Xylene II for 10 min; gradient ethanol rehydration (100% → 95% → 80% → 70%), followed by rinsing with distilled water; Nucleus staining: Harris hematoxylin solution for 6 min, rinsed with tap water and returned to blue for 10 min; 1% hydrochloric acid alcohol for 3 seconds, then rinsed under running water; Cytoplasm staining: 0.5% eosin solution for 1.5 min; gradient ethanol dehydration, xylene clearing, and sealing with neutral gum and coverslip.

Reagents and kits：

10% Neutral Buffered Formalin Fixation Solution Catalog Number: G1101 Manufacturer: Wuhan Servicebio Biotechnology Co., Ltd. Production City: Wuhan, Hubei Province Country: China

Low-melting-point pathological paraffin wax with a melting point of 56–58°C; Catalog number: 39601095; Manufacturer: Leica Biosystems; Production city: Richmond; Country: United States.

Ethanol and Xylene Catalog Numbers: G1119 (Ethanol), G1122 (Xylene); Manufacturer: Wuhan Servicebio Biotechnology Co., Ltd.; Production City: Wuhan;Hubei Province Country: China.

HE Staining Kit Catalog Number: G1005 Manufacturer: Wuhan Servicebio Biotechnology Co., Ltd. Production City: Wuhan, Hubei Province Country: China Kit Components: Harris hematoxylin solution, 1% hydrochloric acid-alcohol differentiation solution, eosin dye solution, lithium carbonate blue fixative solution

### *2.7 Bioinformatics and Target Prediction*

Differential metabolite screening primarily involves Variable Importance in the Projection (VIP), Fold Change (FC), and *p*-value. VIP of the principal component of the PLS-DA model represents the contribution of metabolites to the grouping.[12] FC is the ratio of the mean quantitative values of each metabolite in the comparison group.[13] The *p*-value, indicates the significance level of the differences. The threshold was set as VIP $\geq$ 1.0, FC $\geq$ 2 or FC $\leq$ 0.5, and *p*-value $\leq$ 0.05,FDR < 0.05.[14-17] In **Figure 4**, it indicates the number of differential metabolites present in the different experimental and control groups.

Exogenous xenobiotics and pharmaceutical metabolites were annotated by cross-referencing the exact mass, InChIKey and molecular formula of compounds identified via Compound Discoverer 3.3 against the DrugBank database (https://go.drugbank.com/), which contains structural, metabolic, target gene and pharmacological information for approved and investigational drugs.

Target genes corresponding to annotated pharmaceutical compounds were retrieved from DrugBank, and subsequent functional annotation, disease association of these genes were performed using GeneCards database (https://www.genecards.org/), which integrates multi-omics evidence from over 150 biomedical resources to characterize human gene biological roles systematically.

## 3 Results

### *3.1 QC Samples*

QC samples were prepared by mixing equal volumes of experimental samples and analyzed. Various chromatographic peaks were detected in the QC samples, confirming the stability and reliability of the detection process. After the detection of QC samples the Pearson correlation coefficients (r) between all five QC replicates exceeded 0.98, demonstrating excellent analytical stability and reproducibility of the LC-MS platform. (**Figure 1**)

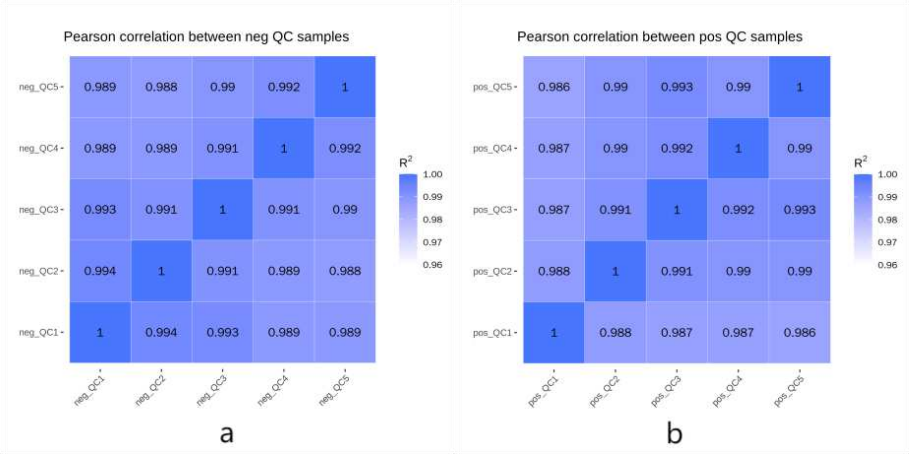
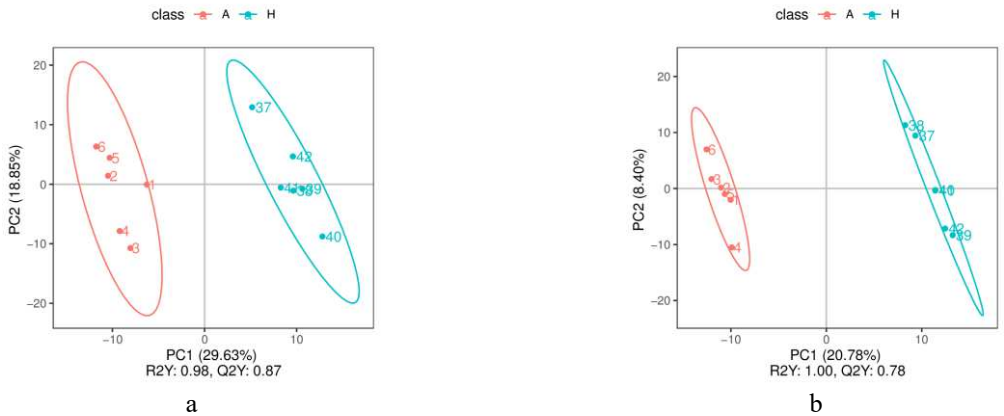
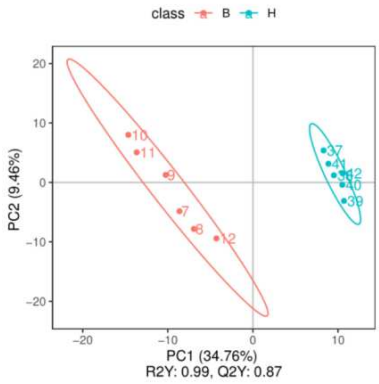



**Figure 1:** Pearson correlation analysis of Quality Control (QC) samples. (a) Negative ion mode. (b) Positive ion mode.

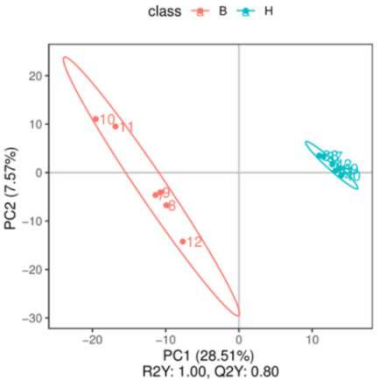
### *3.2 Principal Component Analysis (PCA)*

In the figure2, the horizontal coordinate is the main component 1, and the vertical coordinate is the main component 2. Through the analysis of the two components, the experimental group and the control group can be separated well. (**Figure 2**).The metabolic profiles of Group H can be clearly distinguished from those of Groups A, B, C, D, E, and G, indicating significant inter-group metabolic differences. Samples within each group are tightly clustered, and the six replicates in each experimental group demonstrate good reproducibility; the two replicates in Group H are also closely positioned, confirming the reliability of the sample stability. The absence of crossing 95% confidence ellipses provides strong evidence for the effective separation of groups as determined by PCA.

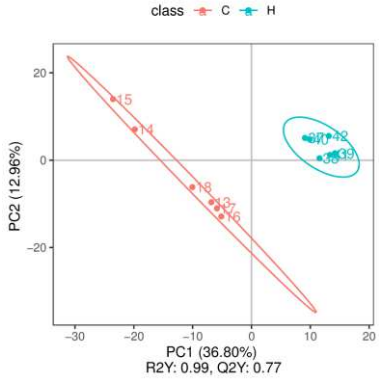



class B H
PC2 (9.46%)
PC1 (34.76%)
R2Y: 0.99, Q2Y: 0.87

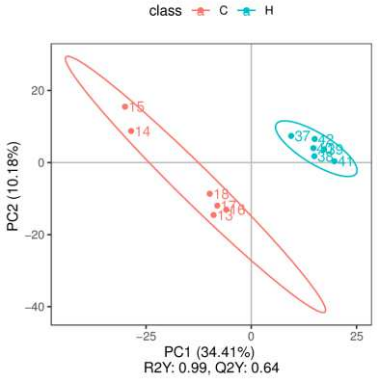
c


class B H
PC2 (7.57%)
PC1 (28.51%)
R2Y: 1.00, Q2Y: 0.80

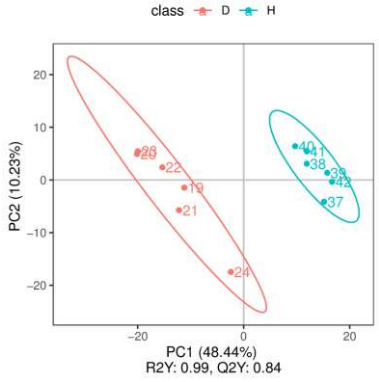
d


class C H
PC2 (12.96%)
PC1 (36.80%)
R2Y: 0.99, Q2Y: 0.77

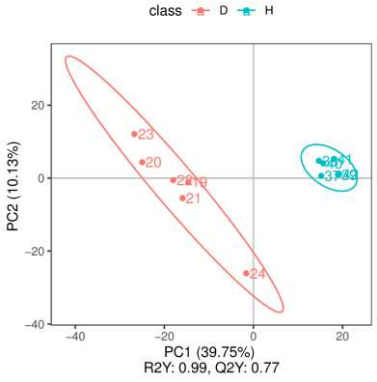
e


class C H
PC2 (10.18%)
PC1 (34.41%)
R2Y: 0.99, Q2Y: 0.64

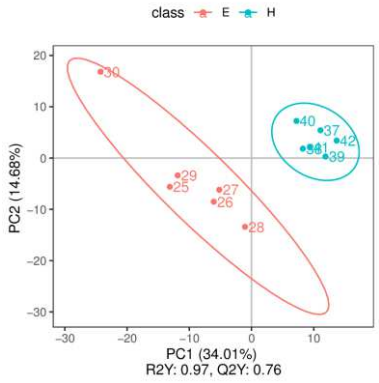
f


class D H
PC2 (10.23%)
PC1 (48.44%)
R2Y: 0.99, Q2Y: 0.84

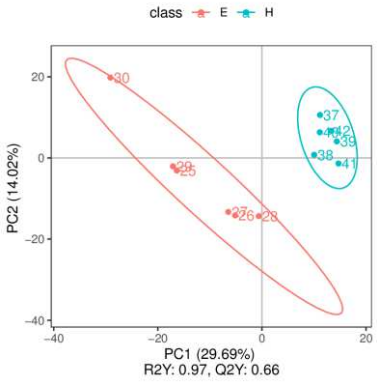
g


class D H
PC2 (10.13%)
PC1 (39.75%)
R2Y: 0.99, Q2Y: 0.77

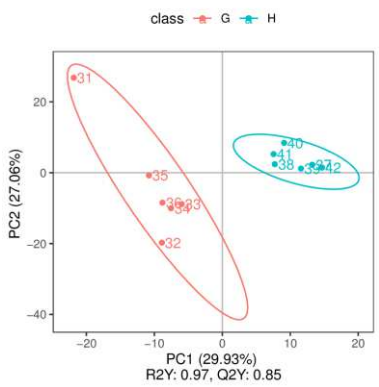
h


class E H
PC2 (14.68%)
PC1 (34.01%)
R2Y: 0.97, Q2Y: 0.76

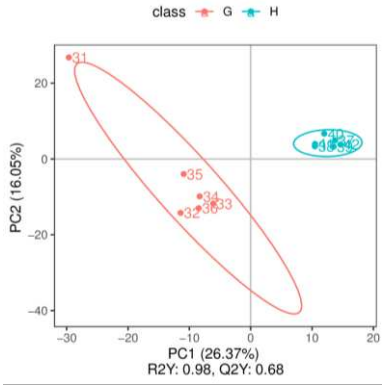
i


class E H
PC2 (14.02%)
PC1 (29.69%)
R2Y: 0.97, Q2Y: 0.66

j




k

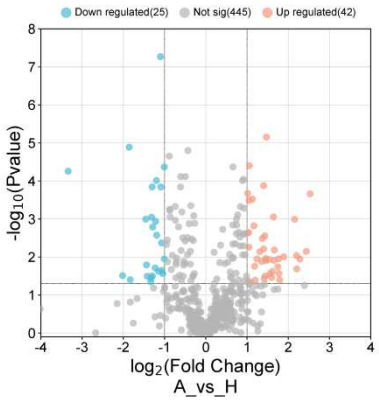



l

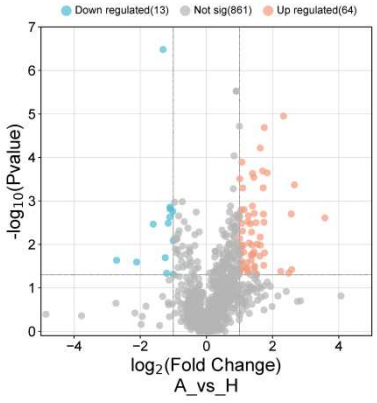
**Figure 2:**Partial least squares discriminant analysis (PLS-DA) score plots of serum metabolites comparing spinal cord injury (SCI) groups at different time points with the sham control group (Group H). Group A (1h) vs. Group H in (a) negative and (b) positive ion modes; Group B (6h) vs. Group H in (c) negative and (d) positive ion modes; Group C (24h) vs. Group H in (e) negative and (f) positive ion modes; Group D (3d) vs. Group H in (g) negative and (h) positive ion modes; Group E (7d) vs. Group H in (i) negative and (j) positive ion modes; and Group G (14d) vs. Group H in (k) negative and (l) positive ion modes.

### *3.3 Differential metabolite screening*

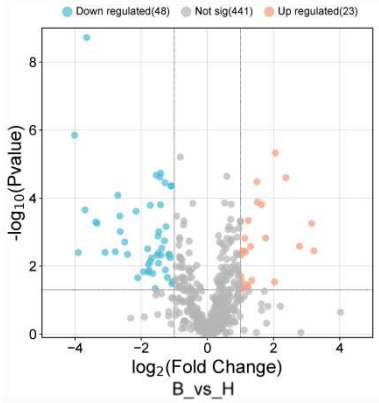
In the volcano map, blue is down regulated differential metabolites, red is up regulated differential metabolites and gray is undifferentiated metabolites. The number in parentheses in the figure is the number of related metabolites. In the Figure 3, the x-axis is $\log_2$(FC) and the y-axis is -$\log_{10}$(*p*-value).

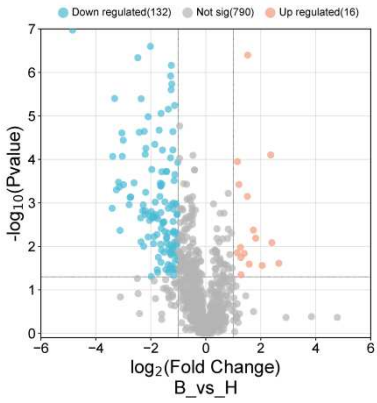



a




b



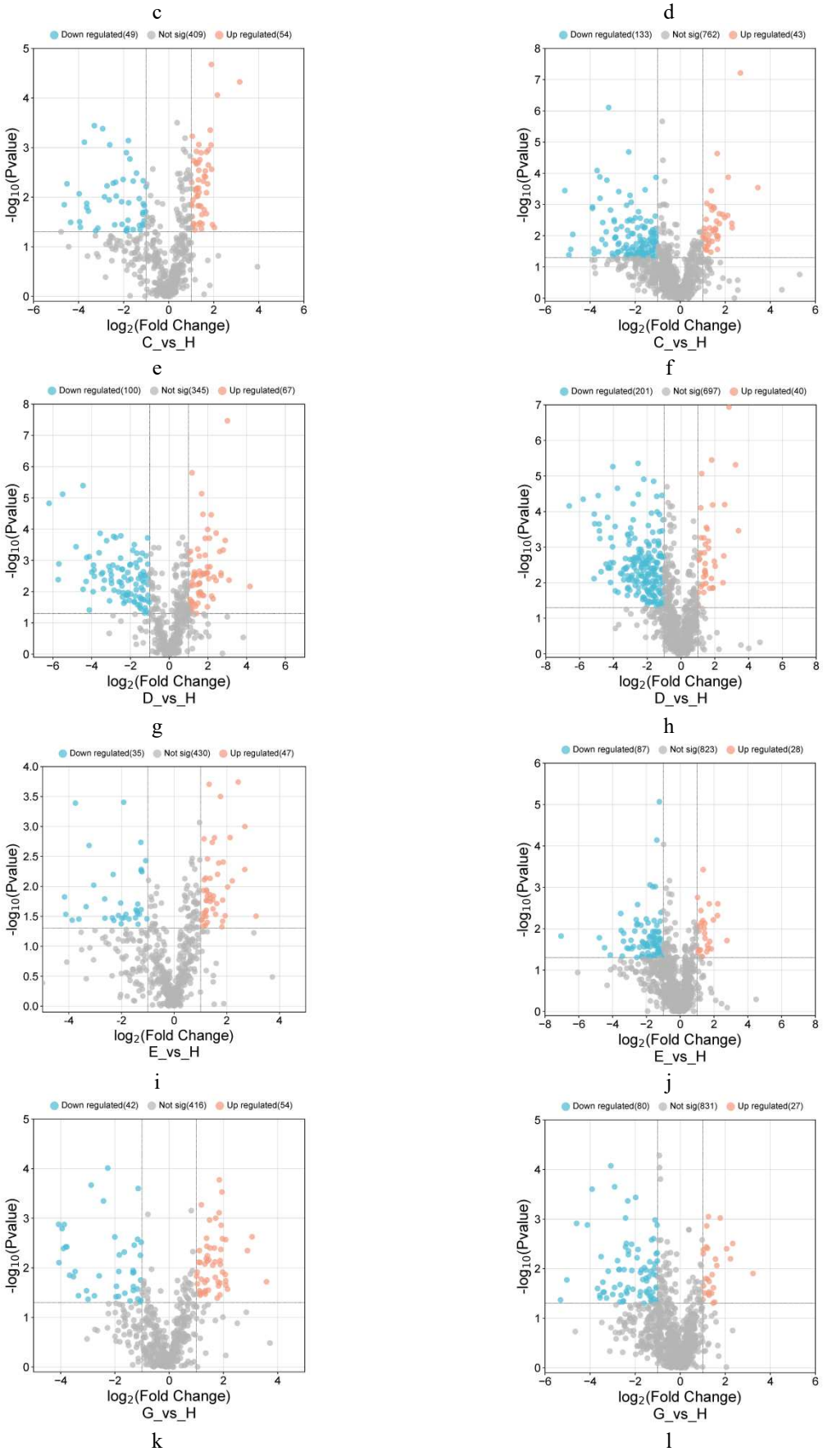



**Figure 3:** Volcano plots of differentially abundant serum metabolites comparing spinal cord injury (SCI) groups at various time points with the sham control group (Group H). Group A (1h) vs. Group H in (a)

negative and (b) positive ion modes; Group B (6h) vs. Group H in (c) negative and (d) positive ion modes; Group C (24h) vs. Group H in (e) negative and (f) positive ion modes; Group D (3d) vs. Group H in (g) negative and (h) positive ion modes; Group E (7d) vs. Group H in (i) negative and (j) positive ion modes; and Group G (14d) vs. Group H in (k) negative and (l) positive ion modes. Red dots represent significantly up-regulated metabolites, blue dots represent significantly down-regulated metabolites, and gray dots represent non-significant metabolites. The numbers in parentheses indicate the counts of corresponding altered metabolites.

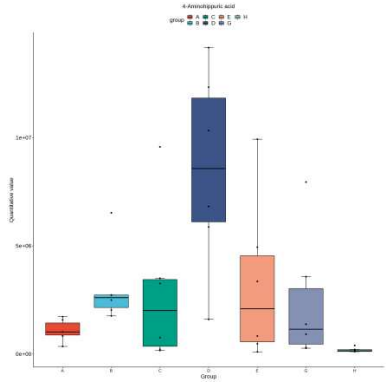
Through experimental assays, we obtained relevant data for eight metabolites. Identification of eight metabolites is listed in samples by LC-MS. (Table 1)

**Table 1:** Identification of eight compounds in samples by LC-MS.

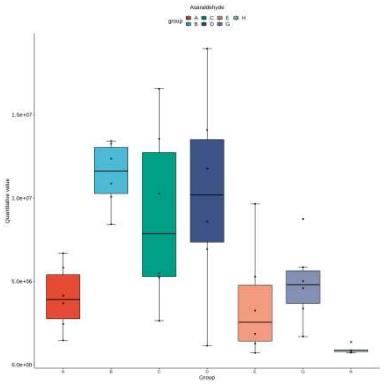
| Name | Formula | Molecular Weight | RT [min] | m/z |
|---|---|---|---|---|
| Asaraldehyde | $C_{10}H_{12}O_4$ | 196.07 | 5.240 | 195.06 |
| 4-Aminohippuric acid | $C_9H_{10}N_2O_3$ | 194.06 | 5.003 | 193.06 |
| 4-(octyloxy)benzoic acid | $C_{15}H_{22}O_3$ | 250.15 | 6.767 | 249.14 |
| Syringic acid | $C_9H_{10}O_5$ | 198.05 | 4.956 | 197.04 |
| 23-Norcholic acid | $C_{23}H_{38}O_5$ | 394.27 | 6.276 | 393.26 |
| Xanthurenic acid | $C_{10}H_7NO_4$ | 205.03 | 5.237 | 204.02 |
| 3-Hydroxy anthranilic acid | $C_7H_7NO_3$ | 153.04 | 1.385 | 154.05 |
| 4-acetyl-4-(ethoxycarbonyl)heptanedioic acid | $C_{12}H_{18}O_7$ | 274.10 | 3.682 | 275.11 |

RT, retention time.

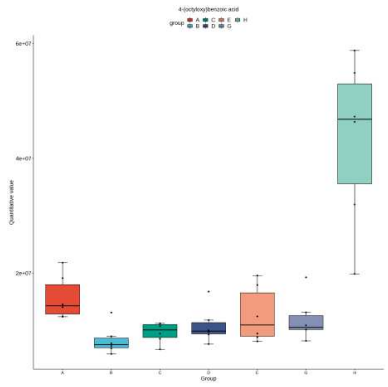
Statistical analysis and control comparisons revealed the following eight metabolites in different experimental groups: asaraldehyde, 4-Aminohippuric acid, 4-(octyloxy)benzoic acid, syringic acid, 23-Norcholic acid, Xanthurenic acid, 3-Hydroxy anthranilic acid (3-HANA), and 4-acetyl-4-(ethoxycarbonyl)heptanedioic acid. In the Figure 4, the x-axis is the name of different experimental groups and control groups, and the y-axis is the metabolite content.



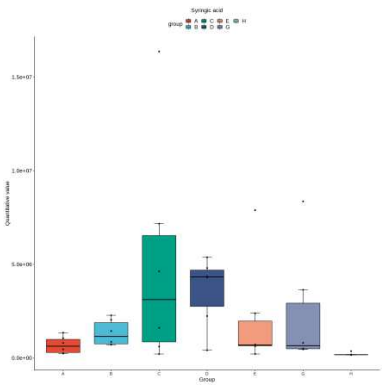
a



b



c



d

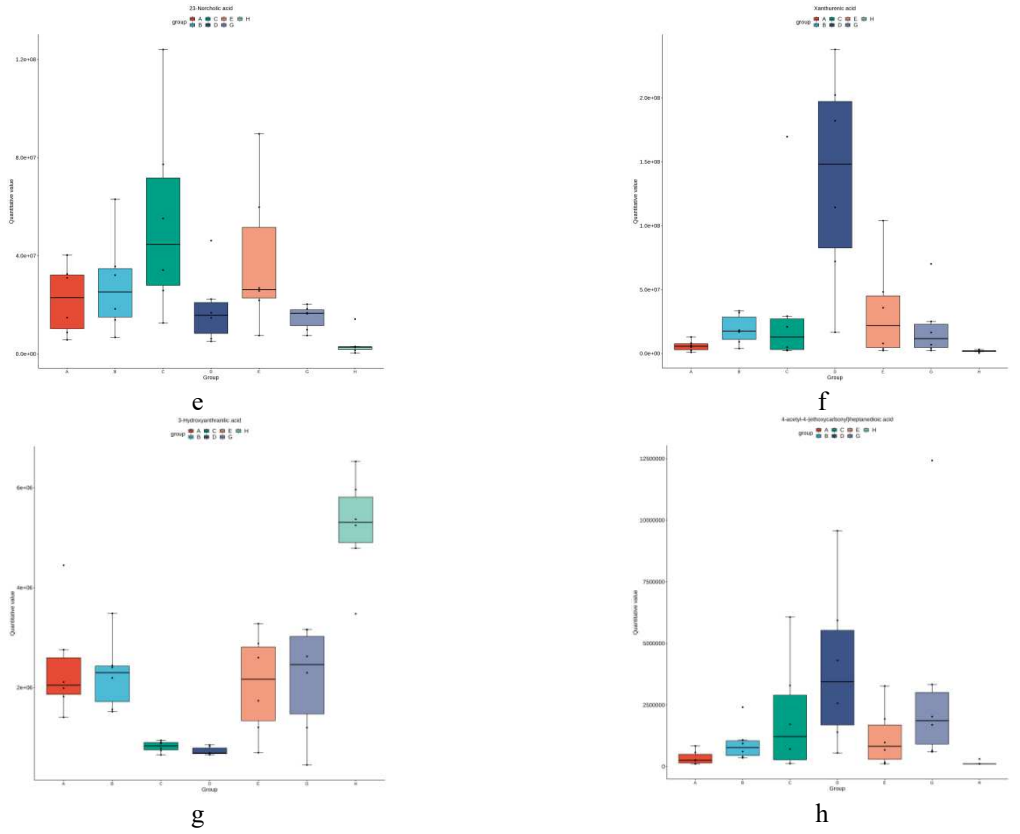



**Figure 4:** Temporal alterations of significantly altered serum metabolites in rats across various post-injury time points compared with the sham control group (Group H): (a) 4-aminohippuric acid, (b) asaraldehyde, (c) 4-(octyloxy)benzoic acid, (d) syringic acid, (e) 23-norcholic acid, (f) xanthurenic acid, (g) 3-hydroxyanthranilic acid (3-HANA), and (h) 4-acetyl-4-(ethoxycarbonyl)heptanedioic acid.

### *3.4 Bladder muscle function*

Following the Mechanical Distraction Stimulation Experiment of Muscle Strips, it was observed that the bladder muscle activity in rats changed to varying degrees. We counted the bladder activity data including the frequency of the bladder muscle contraction (CF), the average contraction force (ACF), and the maximum contraction force (MCF) of each group. CF unit is contractions/min. ACF and MCF unit is gram.We used a tension measuring instrument to detect the contraction amplitude of the bladder muscle and measured the tension threshold. The final value was taken as the average. (**Table 2**)

**Table 2:** Data on bladder activity.

| | CF (contractions/min) | ACF (g) | MCF (g) |
|---|---|---|---|
| Group H (n=36) | 6.54±1.11 | 0.112±0.010 | 0.204±0.055 |
| Group A (n=6) | 7.50±1.41 | 0.182±0.023 | 0.214±0.050 |
| Group B (n=6) | 4.00±0.27 | 0.204±0.012 | 0.291±0.041 |
| Group C (n=6) | 0.00 | 0.00 | 0.00 |
| Group D (n=6) | 3.43±0.29 | 0.510±0.042 | 0.545±0.123 |
| Group E (n=6) | 7.06±1.25 | 0.300±0.084 | 0.360±0.278 |
| Group G (n=6) | 1.60±0.02 | 0.282±0.222 | 0.335±0.324 |

Note: Data are expressed as Mean ± SD. the frequency of the bladder muscle contraction (CF), the average contraction force (ACF), and the maximum contraction force (MCF).

Following spinal cord injury, rats may enter a spinal shock state within 24 hours, leading to the disappearance of the contractile response of the bladder smooth muscle. Beside neural control, the mucosa can also exert a significant influence on the state of the detrusor muscle;

under mechanical, chemical, hormonal, or thermal stimuli, the mucosa can secrete various bioactive substances, including ATP, acetylcholine, nitric oxide, prostaglandins, and neuropeptides, which exert pronounced effects on the detrusor muscle state. HE staining results demonstrate that in the spinal cord injury group, the bladder tissue exhibits marked mucosal loss within the first 24 hours post-injury, with the mucosa nearly completely disappearing by the 24-hours. The absence of these bioactive substances resulting from mucosal loss may also contribute to the abnormal contractile state of the detrusor muscle. Therefore, the spinal shock state following spinal cord injury may be the primary reason for the negative mechanical stretch response observed in isolated detrusor muscles of rats at 24 hours post-injury, while the regulatory factors released by the mucosa may represent a secondary contributing factor to this negative response[18-19](**Figure 5**). Subsequently, we performed a group-matching analysis comparing the bladder contraction data from each experimental group with the eight metabolites identified as significantly differentially expressed through correlation analysis; the results revealed that 3-HANA and Syringic acid were correlated with both the average contraction force (ACF) and the maximum contraction force (MCF) of the bladder.Therefore, we further investigated the targeted pathways of both substances versus the neurogenic bladder. We found 111 targeted gene targets shared by 3-HANA with the neurogenic bladder including response to decreased oxygen levels; spinal cord injury; inflammatory response etc. We found 104 gene targets shared by syringic acid with the neurogenic bladder including regulation of smooth muscle cell proliferation; response to decreased oxygen levels etc. The drugbank (https://go.drugbank.com/) and genecards (https://www.genecards.org/) databases were used to screen for related targets of 3-HANA and syringic acid with neurogenic bladder. The main associated targets of 3-HANA and syringic acid with neurogenic bladder were assessed by Venn plot (**Figure 6, 7**).

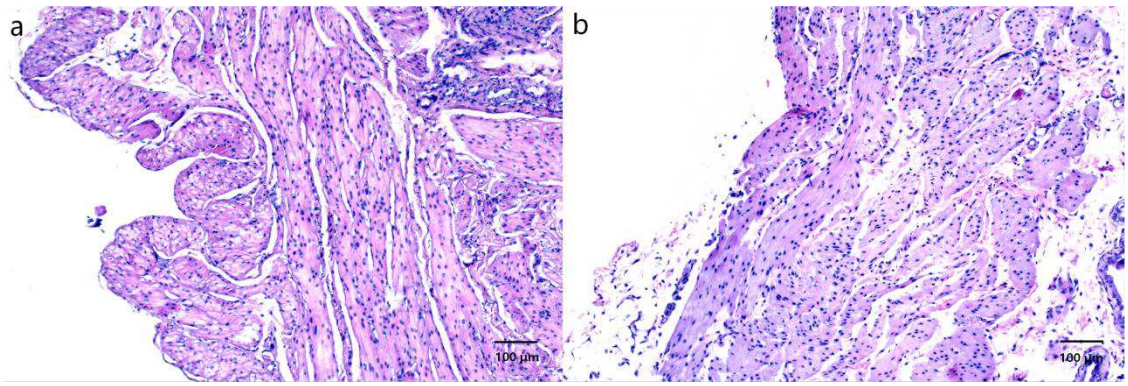



**Figure 5:**(a) Normal intact bladder tissue with complete histological structure, comprising a full mucosal layer, submucosal layer, muscular layer, and serosal layer; the tissue architecture is well-defined with intact cellular structures; (b) Bladder tissue samples for 24 hours exhibit no structural features of bladder mucosal epithelium, retaining only the submucosal and muscular layers.

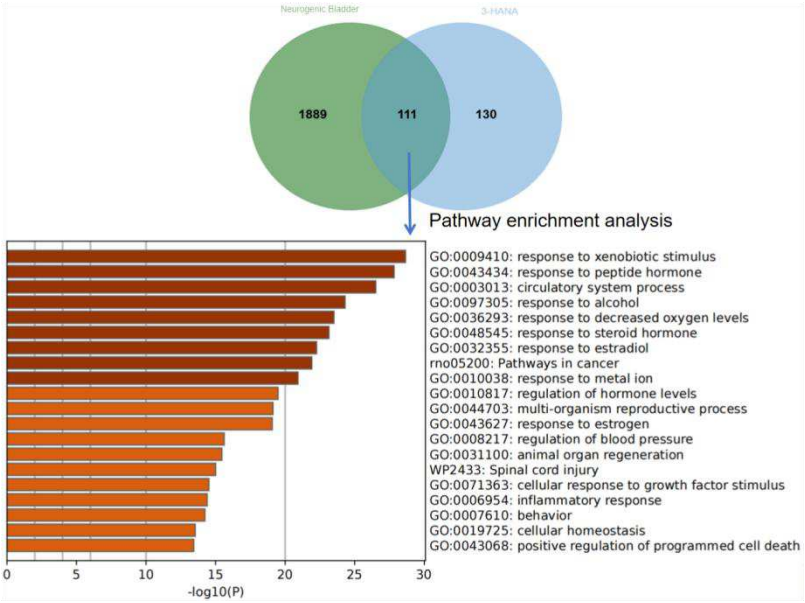



**Figure 6:** 3-HANA possible molecular mechanisms influencing neurogenic bladder.

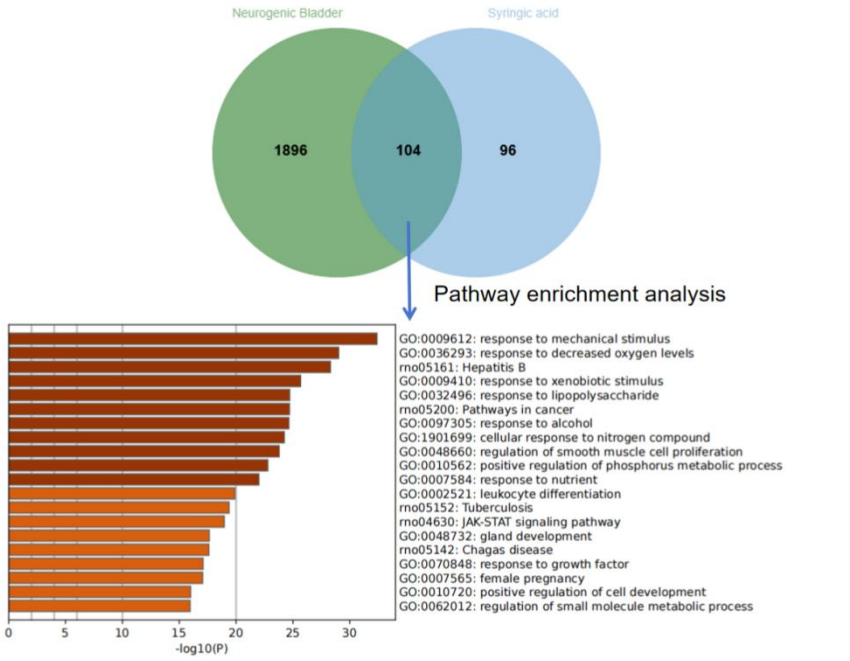



**Figure 7:** Syringic acid possible molecular mechanisms influencing neurogenic bladder.

KEGG analysis showed that 3-HANA was involved in a higher abundance of tryptophan metabolic pathways.（**Figure 8**）

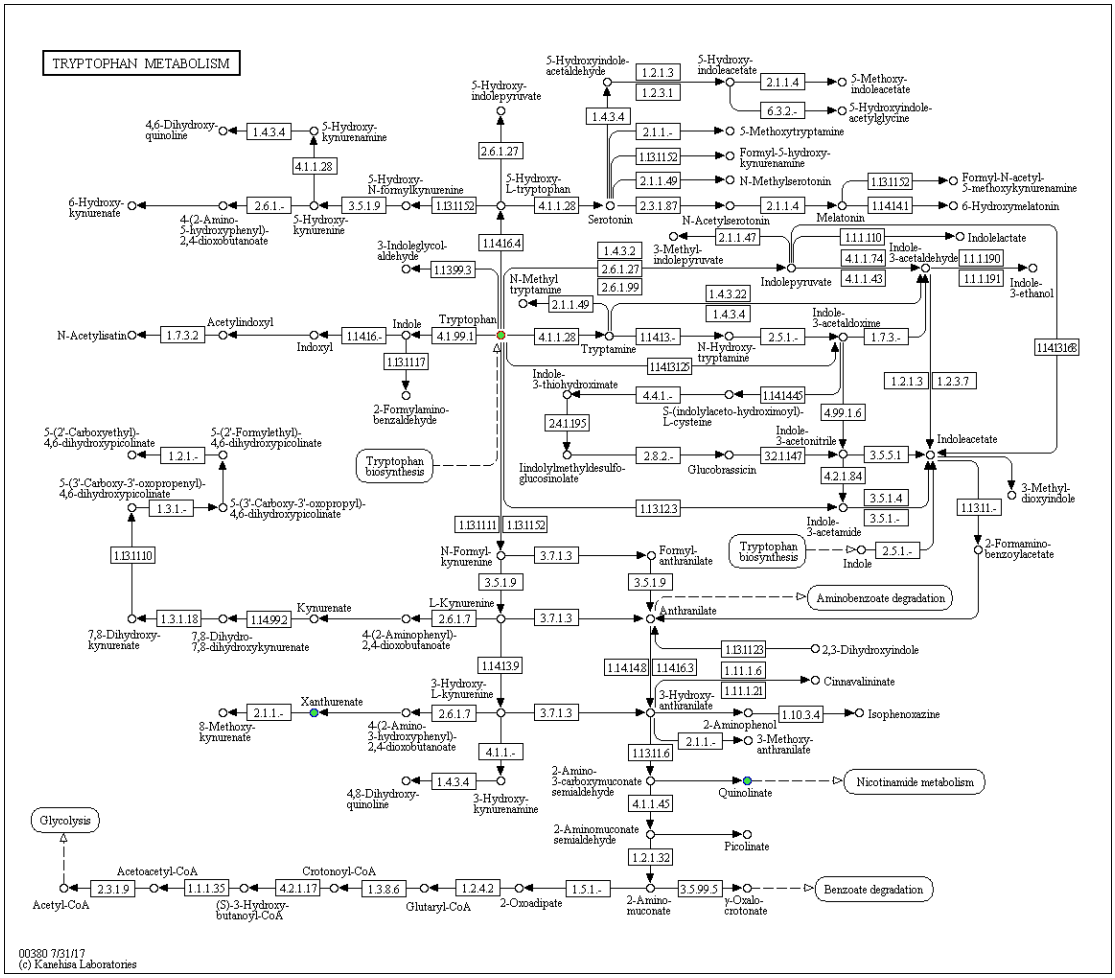



**Figure 8:** tryptophan metabolic pathways.

## 4 Discussion

In this study, we compared different time points groups with a control group. Eight metabolites showed significant differences from the control group across various experimental groups.

The changes in these eight metabolites were observed in seven groups. The levels of 4-(octyloxy)benzoic acid and 3-Hydroxy anthranilic acid were reduced in the experimental group compared to the control group. In contrast, the levels of asaraldehyde, 4-Aminohippuric acid, syringic acid, 23-norcholic acid, Xanthurenic acid, and 4-acetyl-4-(ethoxycarbonyl)heptanedioic acid were increased.

Current literature has demonstrated that Asaraldehyde inhibits the progression of non-small cell lung cancer by inducing ferroptosis and suppressing the PI3K-AKT signaling pathway.[20-21] Abnormal metabolism of 4-Aminohippuric acid has been linked to kidney disease by plasma potassium, suggesting that SCI affects bladder function through the kidneys.[22] The metabolism of 4-(octyloxy)benzoic acid has not been studied in organisms. Numerous in vitro and in vivo studies have evaluated syringic acid's effects on oxidative stress and inflammatory parameters, showing its efficacy in relieving metabolic risk factors, hyperglycemia, hypertension, and hyperlipidemia.[23] Abnormalities in 23-norcholic acid may indicate altered gastrointestinal function in rats after SCI.[24] Regarding xanthurenic acid, literature suggests that xanthurenic acid in the brain may act as a homeostatic signal between the periphery and several brain regions, easily accumulating after peripheral administration. Thus, the status of Xanthurenic acid in certain psychotic or neurodegenerative disorders appears to be specifically related to the brain. The balance of its formation and peripheral input may indicate that the link between the spinal cord and brain after SCI involves changes in

metabolic pathways.[25-26] The sensitivity of 3-hydroxy anthranilic acid (3-HANA) to oxidation could explain its decrease in the experimental group. These observations may further elucidate why 3-HANA levels are reduced in patients with certain neurological disorders and other diseases often associated with elevated ROS concentrations.[27-28] The compound 4-acetyl-4-(ethoxycarbonyl)heptanedioic acid has been less studied.

Additionally, we performed post-hoc tests of all data obtained using one-way ANOVA. To further analyze the significance of these eight metabolites over time, we found a significant difference in the content of 4-acetyl-4-(ethoxycarbonyl)heptanedioic acid between the 1-hour and 14-day groups. Asaraldehyde content showed a significant difference between the 6-hour and 14-day groups. Analysis between the 24-hour and 14-day groups revealed significant differences in 23-norcholic acid content. Significant differences in 4-Aminohippuric acid, Xanthurenic acid, and 3-hydroxy anthranilic acid were observed between the 3-day and 14-day groups. The metabolic pathways involving these substances in the metabolic status of rats after SCI may also change over time.

In the current study, we combined the assessment of bladder function after SCI and found that changes in these substances may also be associated with bladder motility impairment. We matched the material change data of 8 metabolites to bladder function, and finally found that 3-HANA and syringic acid were correlated with the contraction amplitude of bladder. In addition, we further investigated the targets of 3-HANA and syringic acid which were shared with the neurogenic bladder.

Although we performed a comprehensive metabolomic analysis of the collected serum samples, our study has some limitations. First, the sample size is small and requires scale-up for further validation. Second, we did not perform clinical experimental validation to confirm our results. Finally, further studies on differential metabolite screening and metabolic pathways are needed to elucidate the key pathogenic metabolites and their mechanisms.

Through untargeted metabolic analysis of blood in SCI rats, our study offers new strategies for screening biomarkers and understanding mechanisms of SCI progression. It also identifies potential treatment targets. For instance, the differential metabolites we identified could serve as marker molecules for SCI. Our study identified eight differentially expressed metabolites:asaraldehyde, 4-Aminohippuric acid，4-(octyloxy)benzoic acid，syringic acid，23-Norcholic acid， Xanthurenic acid， 3-Hydroxy anthranilic acid (3-HANA)， 4-acetyl-4-(ethoxycarbonyl)heptanedioic acid. The metabolic pathways involving 3-Hydroxy anthranilic acid (3-HANA) and syringic acid may be associated with the occurrence and development of neurogenic bladder. Additionally, we focused on the temporal alterations of these metabolites. Future studies will further explore and elucidate the pathogenesis of induced bladder dysfunction following SCI.

## 5 Conclusions

This study identified a group of serum metabolites that undergo dynamic changes following SCI, among which 3-HANA and Syringic acid are potential biomarkers associated with bladder muscle dysfunction. These metabolites may serve as future research targets for understanding bladder dysfunction related to SCI and provide novel therapeutic intervention strategies.

Future research can be advanced synergistically from three perspectives: continuously deepening the understanding of the underlying molecular mechanisms urinary circuit remodeling and bladder fibrosis following spinal cord injury, and refining the regulatory networks of key signaling pathways; conducting hierarchical validation of candidate targets using large animal models and clinical cohorts to determine the optimal therapeutic window and benefit indications for different disease stages; and performing high-throughput drug screening focused on established targets to identify small-molecule compounds that readily cross the blood-spinal cord barrier while exhibiting both neuroregulatory and anti-fibrotic activities, concurrently optimizing gene and stem cell-based therapies, and exploring staged

combination treatment regimens to achieve the translational goal of delaying or even reversing bladder function impairment.

**Institutional Review Board Statement:** This study was approved by the Animal Experimentation Ethics Committee of Shanxi Medical University and was in accordance with the National Academy of Sciences Guide for the Care and Use of Laboratory Animals (IRB: DWYJ-2024-091).

**Conflicts of Interest:** The authors declare no conflicts of interest.

**Funding:** This research was funded by the Science and Technology Department of Shanxi Province grants 202104041101035. This research was funded by the National Natural Science Foundation of China grants 82470809.

**AUTHOR Contributors:** Yinbo Kang, Yi Rong, Jie Wen, have contributed equally to this work; Yinbo Kang and Weibing Shuang contributed to design the experiment, complete the writing of the article and all the analysis processes; Yi Rong, Yinbo Kang, Jie Wen, Qian Gong and Wenlong Zhang contributed to perform most of the experiments; Dingyang Lv, Huiyu Zhou and Ke Sun assisted in statistical and revision of the article; Weibing Shuang contributed to revise the article and provided guidance for the whole study.

**Data Availability Statement:** The data presented in this study are available on request from the corresponding author..

**Originality: Copyright & Publication Declaration:** This manuscript is original research that has not been published previously, is not under concurrent consideration by any other journal, and no duplicate versions have been posted to preprint servers without full editorial disclosure. All cited materials and reproduced figures/tables have obtained formal copyright permission from the original publishers. No portions of this work contain plagiarized content, and all sources are fully cited. All authors consent to transfer copyright to “The Canadian Journal of Urology” upon acceptance for print and digital publication.

## References

[1]Lu Y ,Shang Z ,Zhang W , et al.Global incidence and characteristics of spinal cord injury since 2000-2021: a systematic review and meta-analysis.[J].BMC medicine,2024,22(1):285.

[2]J D D ,M C M ,A K M , et al.System Failure: Systemic inflammation following spinal cord injury.[J].European journal of immunology,2023,54(1):e2250274-e2250274.

[3]Tate Denise G,Wheeler Tracey,Lane Giulia I, et al.Recommendations for evaluation of neurogenic bladder and bowel dysfunction after spinal cord injury and/or disease[J].J Spinal Cord Med,2020,43(2):141-164.

[4]Chiara P ,M T K .Prediction of Lower Urinary Tract, Sexual, and Bowel Function, and Autonomic Dysreflexia after Spinal Cord Injury.[J].Biomedicines,2023,11(6)

[5]Liu Ying-Hao,Gong Qian,Wang Yi-Kai, et al.Time-Dependent Changes in the Bladder Muscle Metabolome After Traumatic Spinal Cord Injury in Rats Using Metabolomics[J].Int Neurourol J,2023,27(2):88-98.

[6]Fu Y ,Shao Y ,Shen Y .Pharmacokinetic, Bioavailability, and Excretion Study of Hypaphorine Following Intragastric and Intravenous Administration in Rats Using Ultra-High Performance Liquid Chromatography Tandem Mass Spectrometry.[J].Biomedical chromatography : BMC,2026,40(7):e70493.

[7]Establishment and validation of standardized animal models of spinal cord injury by normal external force-caused fracture dislocation[J].Neural Regeneration Research,2011,6(35):2732-2738.

[8]Giannotti A ,Aguinaga M D ,Ferreira A , et al.Animal models of spinal cord injury in neuro-urological research[J].Nature Reviews Urology,2026,(prepublish):1-15.

[9]Xia Xianru,Li Xiandong,Xie Fei, et al.Non-targeted metabonomic analysis of plasma in patients with atherosclerosis by liquid chromatography-mass spectrometry[J].Ann Transl Med,2022,10(3):133.

[10]Wen Bo,Mei Zhanlong,Zeng Chunwei, et al.metaX: a flexible and comprehensive software for processing metabolomics data[J].BMC Bioinformatics,2017,18(1):183.

[11]Pautova K A .Untargeted and Targeted Cerebrospinal Fluid Neurometabolomics via Chromatography–Mass Spectrometry-Based Methods[J].Molecules,2026,31(11):1822-1822.

[12]Chen D ,Colwell N ,Yang Z .Ambient high-spatial-resolution mass spectrometry imaging: recent advances in technologies and metabolomics studies[J].Trends in Analytical Chemistry,2026,198118767-118767.

[13]Shakarami S ,Saleh M N ,Zare F , et al.Integrative proteomics and metabolomics advance early cancer detection and targeted therapy with emerging technologies and clinical applications.[J].Discover oncology,2026,17(1):912-912.

[14]Mo H ,Tian Q ,Li Q , et al.Exploring the Mechanism of Gentiana veitchiorum in Treating Asthma Through Network Pharmacology, Untargeted Metabolomics, and Molecular Docking Technology.[J].Biomedical chromatography : BMC,2026,40(5):e70420.

[15]Xuchen S ,Zhang Y ,Fang S , et al.UHPLC-Q/TOF-MS-based differential metabolite screening and origins classification of Codonopsis Radix[J].Frontiers in Pharmacology,2026,171751079-1751079.

[16]Wang F Z ,You L Y ,Yang G C , et al.Metabolomics analysis using matrix-assisted diffusion-ordered spectroscopy (DOSY) and its application in acrylamide-induced cardiovascular toxicity[J].Microchemical Journal,2024,201110707-.

[17]Iida Miho,Harada Sei,Takebayashi Toru.Application of Metabolomics to Epidemiological Studies of Atherosclerosis and Cardiovascular Disease[J].J Atheroscler Thromb,2019,26(9):747-757.

[18]Vasilakaki S, Barbayianni E, Magrioti V, Pastukhov O, Constantinou-Kokotou V, Huwiler A, Kokotos G. Inhibitors of secreted phospholipase A2 suppress the release of PGE2 in renal mesangial cells [J] . Bioorg Med Chem, 2016, 24(13): 3029-3034.

[19] Stromberga Z, Chess-Williams R, Moro C. The five primary prostaglandins stimulate contractions and phasic activity of the urinary bladder urothelium, l

[20]Chen F ,Chen Y ,Sun W , et al.Anti-PDGFRα autoantibody – a novel diagnostic and prognostic marker – may mediate non-small cell lung cancer progression via the PI3K/AKT/NF-κB signaling pathway[J].British Journal of Cancer,2026,(prepublish):1-13.

[21]Yin H ,Hu Z ,You R Z , et al.Asaraldehyde suppresses non-small cell lung cancer progression via ferroptosis induction and inhibition of PI3K-AKT signaling.[J].American journal of cancer research,2025,15(10)4276-4290.

[22]Sandra W ,Marie M ,Martin F , et al.Correction to: Association of plasma potassium with mortality and end-stage kidney disease in patients with chronic kidney disease under nephrologist care - The NephroTest study.[J].BMC nephrology,2017,18(1):308..

[23]Bartel Iga,Mandryk Izabela,Horbańczuk Jarosław O, et al.Nutraceutical Properties of Syringic Acid in Civilization Diseases-Review[J].Nutrients,2023,16(1):10.

[24]Liu X ,Yu J ,Liu J , et al.Norcholic Acid Promotes M1 Macrophage Polarization in Acute Pancreatitis by Activating the Wnt/β-Catenin Pathway.[J].Frontiers in bioscience (Landmark edition),2025,30(6):39259.

[25] Maitre Michel,Taleb Omar,Jeltsch-David Hélène, et al.Xanthurenic acid: A role in brain intercellular signaling[J].J Neurochem,2024.

[26]Roussel G ,Bessede A ,Klein C , et al.Xanthurenic acid is localized in neurons in the central nervous system[J].Neuroscience,2016,329226-238.

[27]Chobot Vladimir,Hadacek Franz,Weckwerth Wolfram, et al.Iron chelation and redox chemistry of anthranilic acid and 3-hydroxyanthranilic acid: A comparison of two structurally related kynurenine pathway metabolites to obtain improved insights into their potential role in neurological disease development[J].J Organomet Chem,2015,782:103-110.

[28]Zhao H ,Can Z ,JiaXing L , et al.Targeting Mitochondrial Oxidative Stress: Potential Neuroprotective Therapy for Spinal Cord Injury.[J].Journal of integrative neuroscience,2023,22(6):153-153.